



# HHS Public Access

Author manuscript

*Org Biomol Chem.* Author manuscript; available in PMC 2023 October 23.

Published in final edited form as:

*Org Biomol Chem.* ; 20(45): 8833–8837. doi:10.1039/d2ob01931k.

## Mutation of the eunicellane synthase Bnd4 alters its product profile and expands its prenylation ability

Baofu Xu<sup>1</sup>, Wenbo Ning<sup>1</sup>, Xiuting Wei<sup>1</sup>, Jeffrey D. Rudolf<sup>1</sup>

<sup>1</sup>Department of Chemistry, University of Florida, Gainesville, Florida 32611-7011, United States

### Abstract

Bnd4 catalyzes the first committed step in the biosynthesis of the bacterial diterpenoid benditerpenoic acid and was the first eunicellane synthase identified from nature. We investigated the catalytic roles of the aromatic residues in the active site of Bnd4 through a series of mutation studies. These experiments revealed that large hydrophobic or aromatic side chains are required at F162 and Y197 for eunicellane formation and that selected mutations at W316 converted Bnd4 into a cembrane synthase. In addition, the Bnd4<sup>Y197A</sup> variant expanded the native prenylation ability of Bnd4 from accepting C<sub>5</sub> and C<sub>10</sub> prenyl donors to C<sub>15</sub>. This study supports the mechanism of eunicellane formation by Bnd4 and encourages further engineering of terpene synthases into practical and efficient prenyltransferases.

Terpenoids are the most structurally diverse family of natural products.<sup>1,2</sup> Most terpenoids possess polycyclic carbon skeletons that arise from a family of enzymes, terpene synthases (TSs). TSs use carbocation chemistry to catalyze complex cyclization reactions using acyclic prenyl diphosphates.<sup>3,4</sup> After the initial carbocation is formed, either by diphosphate abstraction (type I TS) or protonation (type II TS), TSs exquisitely control product formation by chaperoning the extremely reactive cation through a series of intermediates before final cation quench. Impressively, TSs guide these reaction cascades, using their hydrophobic and aromatic active sites to stabilize the innately reactive intermediates via cation- $\pi$  interactions,<sup>5–7</sup> to frequently provide a single stereoselective product. All canonical TSs

Corresponding Author jrudolf@chem.ufl.edu.

**Baofu Xu** – Department of Chemistry, University of Florida, Gainesville, Florida 32611-7011, United States; Present Address: Drug Discovery Shandong Laboratory, Bohai Rim Advanced Research Institute for Drug Discovery, Yantai, Shandong, 264117, China; State Key Laboratory of Drug Research, Shanghai Institute of Materia Medica, Chinese Academy of Sciences, Shanghai, 201203, China; University of Chinese Academy of Sciences, Beijing, 100039, China

**Wenbo Ning** – Department of Chemistry, University of Florida, Gainesville, Florida 32611-7011, United States

**Xiuting Wei** – Department of Chemistry, University of Florida, Gainesville, Florida 32611-7011, United States

**Jeffrey D. Rudolf** – Department of Chemistry, University of Florida, Gainesville, Florida 32611-7011, United States

Author Contributions

B.X. and J.D.R. conceived the project and designed the experiments; B.X., W.N., and X.W. performed the experiments; B.X. and J.D.R. analyzed the results; B.X. and J.D.R. wrote the manuscript with input from all co-authors.

The authors declare no competing financial interest.

### ASSOCIATED CONTENT

Supporting Information.

The Supporting Information is available free of charge on the ChemRxiv website.

Methods; strains, plasmids, and primers used in this study (Tables S1–S3); summary of NMR data for compounds **6** and **7** (Table S4); sequence alignments of relevant diterpene synthase (Figures S1 and S23); SDS-PAGE analysis of purified proteins (Figure S2); diterpene overproduction system in *E. coli* (Figure S3); NMR spectra of compounds **2–4**, **6**, **7**, and **9** (Figures S4–S11, S13–22, and S24–27); HPLC traces of enzyme reactions (Figures S12 and S28); supporting references (PDF)

share the same overall structures,<sup>3,8</sup> but their sequence diversities create unsolved challenges in understanding sequence–function relationships.

Recently, benditerpenoic acid, a bacterial eunicellane diterpenoid harboring a 6,10-bicyclic scaffold, was isolated from *Streptomyces* sp. (CL12–4).<sup>9</sup> In collaboration with Prof. Loesgen, we also identified its biosynthetic gene cluster and characterized the first eunicellane-forming TS, Bnd4, which produces benditerpe-2,6,15-triene (**1**) (Figure 1A).<sup>9</sup> We then investigated the mechanism of eunicellane formation through a series of labeling studies, quantum chemical calculations, and mutagenesis experiments.<sup>10</sup> However, key questions remained including how the aromatic residues in Bnd4 assist in controlling cyclization and which, if any, residues are directly involved in final deprotonation to form **1**. We set out to answer those questions with a series of mutation experiments focused on the aromatic residues of Bnd4.

In the Bnd4 model, the active site is lined with five aromatic residues, W67, F162, Y197, W316, and Y323, all of which are within 4 Å of docked geranylgeranyl diphosphate (GGPP) (Figure 1B). These residues are also strictly conserved amongst the eight other Bnd4 homologues (Fig. S1).<sup>9,10</sup> Based on the mechanism of Bnd4, which is supported by isotope labeling studies and quantum chemical calculations, carbocations are sequentially formed on C1, C11, C1, and C15 (Figure 1A).<sup>10</sup> Y323 is positioned near C1 of GGPP (3.1 Å) suggesting it may stabilize either the initial carbocation after diphosphate abstraction or the monocyclic intermediate after the 1,3-hydride shift, or both. W316, W67, Y197, and F162 form one wall of the hydrophobic active site with both Y197 and F162 near the methyl groups on C15. Given the proximity of Y197 to C16 (3.5 Å), we hypothesized that Y197 may act as the base that deprotonates C16 to complete the reaction.

We first performed alanine scanning mutagenesis on the five aromatic residues in the active site. Four of the five variants, Bnd4<sup>F162A</sup>, Bnd4<sup>Y197A</sup>, Bnd4<sup>W316A</sup>, and Bnd4<sup>Y323A</sup>, were soluble (Figure S2); Bnd4<sup>W67A</sup> was insoluble and excluded from further study. In vitro incubation of these Bnd4 variants with GGPP resulted in the appearance of new peaks **2–4** (Figure 2A). Bnd4<sup>Y197A</sup> abolished production of **1** and gave a polar major peak, **3**, and two minor peaks, **2** and **4**; Bnd4<sup>F162A</sup> similarly produced **3** and **4**, but still produced a significant amount of **1**. Bnd4<sup>W316A</sup> produced **1** and several additional minor peaks while the product profile of Bnd4<sup>Y323A</sup> did not change from that of native Bnd4. Considering the proposed location of Y323 near C1 of GGPP, (Figure 1B) it was surprising that Bnd4<sup>Y323A</sup> did not affect cyclization activity.

To facilitate the isolation and structural characterization of enzymatic products, we established a new GGPP overproduction system in *E. coli*. Previously, we employed published GGPP overproduction systems<sup>9,11,12</sup> with varying levels of terpene production and reproducibility. Inspired by recent reports of an artificial pathway for isoprenoid biosynthesis in *E. coli* that leverages two kinases to sequentially phosphorylate exogenously added isoprenol,<sup>13–15</sup> we emulated these systems to establish a reliable GGPP overproduction system. We cloned two kinases, namely hydroxyethylthiazole kinase (ThiM) from *E. coli* and isopentenyl phosphate kinase (IPK) from *Arabidopsis thaliana*, with isopentenyl diphosphate isomerase (IDI) from *E. coli* and a putative GGPP synthase (Bnd3)

from *Streptomyces sp.* (CL12–4)<sup>9</sup> into one operon under control of a single T7 promoter with a ribosome binding site upstream of each gene (pET28a-MKI4 or pJR1064; Figure S3). To test the ability of the MKI4 system to overproduce GGPP, we transformed pET28a-MKI4 into *E. coli* harboring Bnd4. Under the conditions tested, **1** was consistently produced at a titer of 32 mg L<sup>-1</sup> (Figure S3).<sup>9</sup>

With a new GGPP overproduction system in hand, we set out to isolate and identify the new peaks produced by the aforementioned Bnd4 variants. Large-scale (12× 1-L) cultures of *E. coli* strains harboring the MKI4 system with the individual *bnd4* mutants led to the identification of  $\beta$ -springene (**2**), geranylgeraniol (**3**, GGOH), and geranylinalool (**4**) (Figures 2 and S4–11, SI). Both Bnd4<sup>F162A</sup> and Bnd4<sup>Y197A</sup> produced the acyclic terpenes **3** and **4**; however, Bnd4<sup>F162A</sup> retained its ability to form **1** while Bnd4<sup>Y197A</sup> did not (Figure 2B). This suggested that Y197 is an important player in the formation of the eunicellane scaffold. To investigate the role of Y197, we additionally created Bnd4<sup>Y197F</sup> but its cyclization activity was unaffected (Figure 2B). Considering the proximity of F162 to Y197 (Figure 1B), we tested Bnd4<sup>F162Y</sup>, Bnd4<sup>Y197A/F162A</sup>, and Bnd4<sup>Y197F/F162Y</sup>. Retention of aromaticity at 162 and 197 did not negatively affect the formation of **1** while the double Ala variant almost completely abolished all activity. We also mutated Y197 to Trp, His, Met, and Leu and each of these variants showed similar activities to that of native Bnd4 (Figure S12), suggesting that hydrophobicity at Y197 is sufficient to support eunicellane cyclization and deprotonation. Re-inspection of the active site revealed that the backbone carbonyls of L90 and V192 are both less than 3.4 Å away from the methyls on C15.<sup>9</sup> One of these carbonyls may act as the base for final deprotonation of the benditerpe-2,6,15-triene skeleton.<sup>16</sup>

The product profile of Bnd4<sup>W316A</sup> was significantly different than that of the other variants tested. W316 is found within the WxxxxRY motif, which is highly conserved among bacterial diterpene synthases and proposed to guide product formation.<sup>17</sup> W316 was additionally mutated to Tyr, Phe, and His to assess its impact on cyclization. In vitro, Bnd4<sup>W316Y</sup> and Bnd4<sup>W316F</sup> showed activity similar to that of native Bnd4, although the production of **1** slightly decreased (Figure 2C). The product profiles of Bnd4<sup>W316H</sup> paralleled that of Bnd4<sup>W316A</sup>, showing continued production of **1** and the appearance of new peaks **5–8**; products **5** and **7** were the major peaks of Bnd4<sup>W316H</sup> and Bnd4<sup>W316A</sup>, respectively (Figure 2C). Using the MKI4 system, we identified four cembranoids from *E. coli* producing Bnd4<sup>W316A</sup> or Bnd4<sup>W316H</sup>: nephthenol (**5**), cembrene C (**6**), cembrene A (**7**), and the isopropylidene isomer of cembrene C (**8**) (Figures 2 and S13–22, Table S4). Products **5** and **8** were identified by comparison with the known products of DtCycA, a cembrene synthase from *Streptomyces sp.* SANK 60404.<sup>18</sup> The formation of these cembranoids clearly indicates that substitution of W316 perturbs the active site cavity enough to alter the binding orientation of GGPP such that C1 and C14 are in proximity to each other and can form the 14-membered macrocycle directly after diphosphate abstraction.

Only four native bacterial TSs are known to produce the cembrane skeleton and while cembranoids are common in marine organisms, particularly coral,<sup>19</sup> there have been no cembranoid natural products isolated from bacteria;<sup>2</sup> the cyanobacterial tasilalides were speculated to arise from an oxygenated cembrane diterpenoid.<sup>20</sup> DtcycA and DtcycB from

*Streptomyces* sp. SANK 60404 produce (*R*)-**5** and **8** and (*R*)-**5** and (*R*)-(-)-**7**, respectively;<sup>18</sup> the gene product of *rxyl\_0493* from *Rubrobacter xylanophilus* produces **6**,<sup>21</sup> and cembrene A synthase from *Allokutzneria albata* produces (*S*)-(+)-**7**.<sup>22</sup> Interestingly, DtcycA possesses an A<sup>321</sup>xxxxxRY motif in place of the expected WxxxxxRY motif (Figure S23), which made us speculate if DtcycA could be engineered to biosynthesize polycyclic diterpenes such as the eunicellane skeleton through a single A321W mutation. We thus obtained a synthetic *dtcycA* gene and confirmed that DtcycA produces **5** and **8** with minor amounts of **6** and **7** (Figure 2D). Contrary to our hypothesis, the product profile of DtcycA<sup>A321W</sup> did not change from that of native DtcycA indicating that the residue at 321 is not solely responsible for cembrene formation. Additional studies are needed to identify if and how cembrene synthases can be engineered into polycyclic-forming diterpene synthases.

Finally, given our recent finding that bacterial diterpene synthases also catalyze the prenylation of small molecules using prenyl diphosphates that are shorter than their native substrates,<sup>23</sup> we saw an opportunity to assess the prenylation activity of Bnd4 variants to determine if we could expand their ability to perform Friedel-Crafts alkylation.<sup>24,25</sup> Bnd4 and other diterpene synthases such as CotB2 were shown to use both dimethylallyl diphosphate (DMAPP, C<sub>5</sub>) and geranyl diphosphate (GPP, C<sub>10</sub>) as prenyl donors but did not show prenylation activity with farnesyl diphosphate (FPP, C<sub>15</sub>) or GGPP (C<sub>20</sub>).<sup>23</sup> We proposed that the efficient production of GGOH (**3**) by Bnd4<sup>Y197A</sup> provided an active site that may be more amenable to using longer prenyl donors for prenylation. To test this hypothesis, we incubated Bnd4<sup>Y197A</sup> with indole and FPP or GGPP. One major peak, which was determined to be 3-farnesylindole (**9**, Figure S24–27, SI), and a related minor peak was identified after incubation with FPP (Figure 3); indole was not prenylated by GGPP (Figure S28). To evaluate if the corresponding residues of Y197 in other diterpene synthases can expand their prenylation activities, we constructed the CotB2<sup>W186A</sup> variant. As proposed, incubation of indole and FPP with CotB2<sup>W186A</sup> with indole and FPP also resulted in the production of **9** (Figure 3). Previous mutations of W186 in CotB2 resulted in early termination of the cyclization cascade resulting in (*R*)-**7** (W186L), 3,7,18-dolabellatriene (W186L/H), cyclooctat-7-en-3-ol (W186F/H), and 3,7-dolabelladiene-9-ol and cyclooctat-6-en-8-ol (W186F).<sup>17,26,27</sup> This data, along with the formation of **3** by Bnd4<sup>Y197A</sup>, indicates that changes in the active sites of TSs that alter the natural cyclization reactions may provide opportunities to engineer TSs into prenyltransferases.

One of the grand challenges in enzymology is the ability to predict substrate, reaction, and product from protein sequence alone.<sup>28</sup> To realize this goal in terpene enzymology, it is important to understand the roles of amino acids in substrate binding and catalysis to shape general principles of TSs. In this study, we investigated the roles of the aromatic residues in the active site of Bnd4, a bacterial eunicellane synthase. Using mutagenesis and an improved diterpene production system in *E. coli*, we identified that Y197 and W316 are key players for eunicellane formation. In addition, we engineered Bnd4 and CotB2 into prenyltransferases that accept FPP as a prenyl donor, thus expanding the ability of diterpene synthases to prenylate small molecules. Future studies are targeted to better understand how bacterial diterpene synthases control eunicellane formation and stereoselectivity.

## Supplementary Material

Refer to Web version on PubMed Central for supplementary material.

## ACKNOWLEDGMENTS

This work was funded in part by NIH Grants R00 GM124461 and R35 GM142574. We thank Prof. Sandra Loesgen and Prof. Gavin Williams for helpful discussions, and Prof. Loesgen for providing *Streptomyces* sp. (CL12-4). We also thank Prof. Sixue Chen for providing *Arabidopsis* cDNA. We acknowledge the University of Florida Center for Nuclear Magnetic Resonance Spectroscopy for NMR support.

## REFERENCES

- (1). Dictionary of Natural Products, <http://dnp.chemnetbase.com>, accessed April 28, 2022.
- (2). Rudolf JD; Alsup TA; Xu B; Li Z Bacterial terpenome. *Nat. Prod. Rep.* 2021, 38, 905–980. [PubMed: 33169126]
- (3). Christianson DW Structural and chemical biology of terpenoid cyclases. *Chem. Rev.* 2017, 117, 11570–11648. [PubMed: 28841019]
- (4). Dickschat JS Bacterial Terpene Cyclases. *Nat. Prod. Rep.* 2016, 33, 87–110. [PubMed: 26563452]
- (5). Mahadevi AS; Sastry GN Cation- $\pi$  interaction: its role and relevance in chemistry, biology, and material science. *Chem. Rev.* 2013, 113, 2100–2138. [PubMed: 23145968]
- (6). Ronnebaum TA; Gardner SM; Christianson DW An aromatic cluster in the active site of episoizaene synthase is an electrostatic toggle for divergent terpene cyclization pathways. 2020, 59, 4744–4754.
- (7). Hare SR; Pemberton RP; Tantillo DJ Navigating past a fork in the road: carbocation- $\pi$  interactions can manipulate Dynamic behavior of reactions facing post-transition-state bifurcations. *J. Am. Chem. Soc.* 2017, 139, 7485–7493. [PubMed: 28504880]
- (8). Rudolf JD; Chang CY Terpene synthases in disguise: enzymology, structure, and opportunities of non-canonical terpene synthases. *Nat. Prod. Rep.* 2020, 37, 425–463. [PubMed: 31650156]
- (9). Zhu C; Xu B; Adpressa DA; Rudolf JD; Loesgen S Discovery and biosynthesis of a structurally dynamic antibacterial diterpenoid. *Angew. Chem., Int. Ed.* 2021, 60, 14163–14170.
- (10). Xu B; Tantillo DJ; Rudolf JD Mechanistic insights into the formation of the 6,10-bicyclic eunicellane skeleton by the bacterial diterpene synthase Bnd4. *Angew. Chem., Int. Ed.* 2021, 60, 23159–23163.
- (11). Rudolf JD; Dong L. Bin; Cao H; Hatzos-Skintges C; Osipiuk J; Endres M; Chang CY; Ma M; Babnigg G; Joachimiak A; et al. Structure of the *ent*-copalyl diphosphate synthase PtmT2 from *Streptomyces platensis* CB00739, a bacterial type II diterpene synthase. *J. Am. Chem. Soc.* 2016, 138, 10905–10915. [PubMed: 27490479]
- (12). Peralta-Yahya PP; Ouellet M; Chan R; Mukhopadhyay A; Keasling JD; Lee TS Identification and microbial production of a terpene-based advanced biofuel. *Nat. Commun.* 2011., 2, 483. [PubMed: 21952217]
- (13). Lund S; Hall R; Williams GJ An artificial pathway for isoprenoid biosynthesis decoupled from native hemiterpene metabolism. *ACS Synth. Biol.* 2019, 8, 232–238. [PubMed: 30648856]
- (14). Clomburg JM; Qian S; Tan Z; Cheong S; Gonzalez R The isoprenoid alcohol pathway, a synthetic route for isoprenoid biosynthesis. *Proc. Natl. Acad. Sci.* 2019, 116, 12810–12815. [PubMed: 31186357]
- (15). Chatzivasileiou AO; Ward V; Edgar SMB; Stephanopoulos G Two-Step pathway for isoprenoid synthesis. *Proc. Natl. Acad. Sci. U. S. A.* 2019, 116, 506–511. [PubMed: 30584096]
- (16). Wang Y-H; Xu H; Zou J; Chen X-B; Zhuang Y-Q; Liu W-L; Celik E; Chen G-D; Hu D; Gao H; et al. Catalytic role of carbonyl oxygens and water in selinadiene synthase. *Nat. Catal.* 2022, 5, 128–135.
- (17). Driller R; Garbe D; Mehlmer N; Fuchs M; Raz K; Major DT; Brück T; Loll B Current understanding and biotechnological application of the bacterial diterpene synthase CotB2. *Beilstein J. Org. Chem.* 2019, 15, 2355–2368. [PubMed: 31666870]

- (18). Meguro A; Tomita T; Nishiyama M; Kuzuyama T Identification and characterization of bacterial diterpene cyclases that synthesize the cembrane skeleton. *ChemBioChem* 2013, 14, 316–321. [PubMed: 23386483]
- (19). Li G; Dickschat JS; Guo YW Diving into the world of marine 2,11-cyclized cembranoids: a summary of new compounds and their biological activities. *Nat. Prod. Rep.* 2020, 37, 1367–1383. [PubMed: 32458945]
- (20). Williams PG; Yoshida WY; Moore RE; Paul VJ Novel iodinated diterpenes from a marine cyanobacterium and red alga assemblage. *Org. Lett.* 2003, 5, 4167–4170. [PubMed: 14572276]
- (21). Yamada Y; Kuzuyama T; Komatsu M; Shin-ya K; Omura S; Cane DE; Ikeda H Terpene synthases are widely distributed in bacteria. *Proc. Natl. Acad. Sci. U. S. A.* 2015, 112, 857–862. [PubMed: 25535391]
- (22). Rinkel J; Lauterbach L; Rabe P; Dickschat JS Two diterpene synthases for spiroalbatene and cembrene A from *Allokutzneria albata*. *Angew. Chem., Int. Ed.* 2018, 57, 3238–3241.
- (23). Xu B; Li Z; Alsup TA; Ehrenberger MA; Rudolf JD Bacterial diterpene synthases prenylate small molecules. *ACS Catal.* 2021, 11, 5906–5915. [PubMed: 34796043]
- (24). Kumar V; Turnbull WB; Kumar A Review on recent developments in biocatalysts for Friedel-Crafts reactions. *ACS Catal.* 2022, 12, 10742–10763.
- (25). Mori T Enzymatic studies on aromatic prenyltransferases. *J. Natural Med.* 2020, 74, 501–512.
- (26). Tomita T; Kobayashi M; Karita Y; Yasuno Y; Shinada T; Nishiyama M; Kuzuyama T Structure and mechanism of the monoterpene cyclolavandulyl diphosphate synthase that catalyzes consecutive condensation and cyclization. *Angew. Chem., Int. Ed.* 2017, 56, 14913–14917.
- (27). Janke R; Görner C; Hirte M; Brück T; Loll B The first structure of a bacterial diterpene cyclase: CotB2. *Acta Crystallogr. Sect. D Biol. Crystallogr.* 2014, 70, 1528–1537. [PubMed: 24914964]
- (28). Gerlt JA; Allen KN; Almo SC; Armstrong RN; Babbitt PC; Cronan JE; Dunaway-Mariano D; Imker HJ; Jacobson MP; Minor W; et al. The Enzyme Function Initiative. *Biochemistry* 2011, 50, 9950–9962. [PubMed: 21999478]

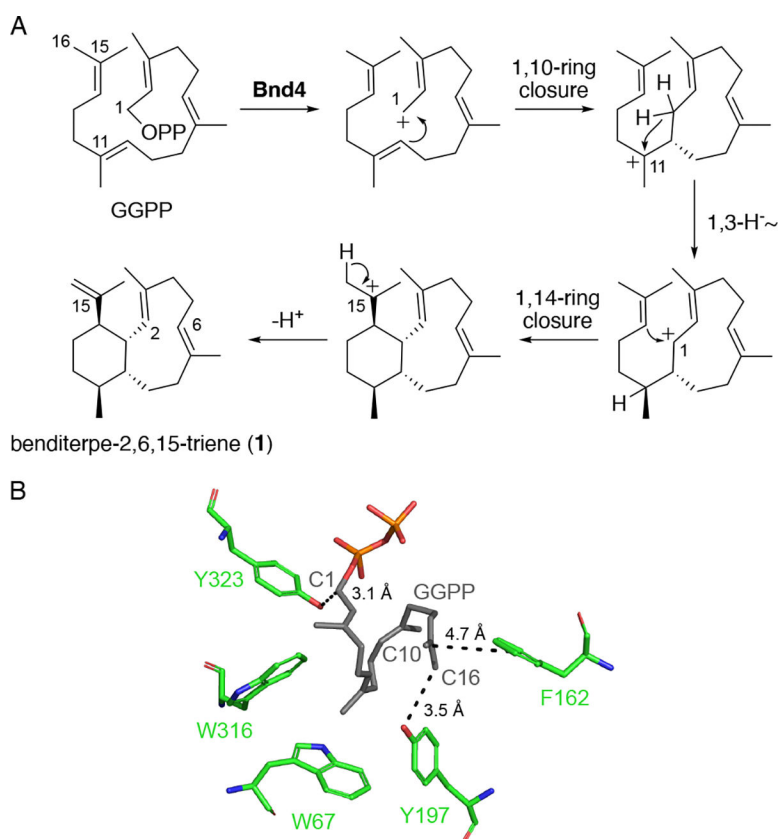


**Figure 1.** (A) Experimentally supported mechanism of eunicellane formation by Bnd4.<sup>10</sup> (B) Structural model of Bnd4 displaying key active site aromatic residues (green) and a docking model of GGPP (grey); dashed lines are distances.

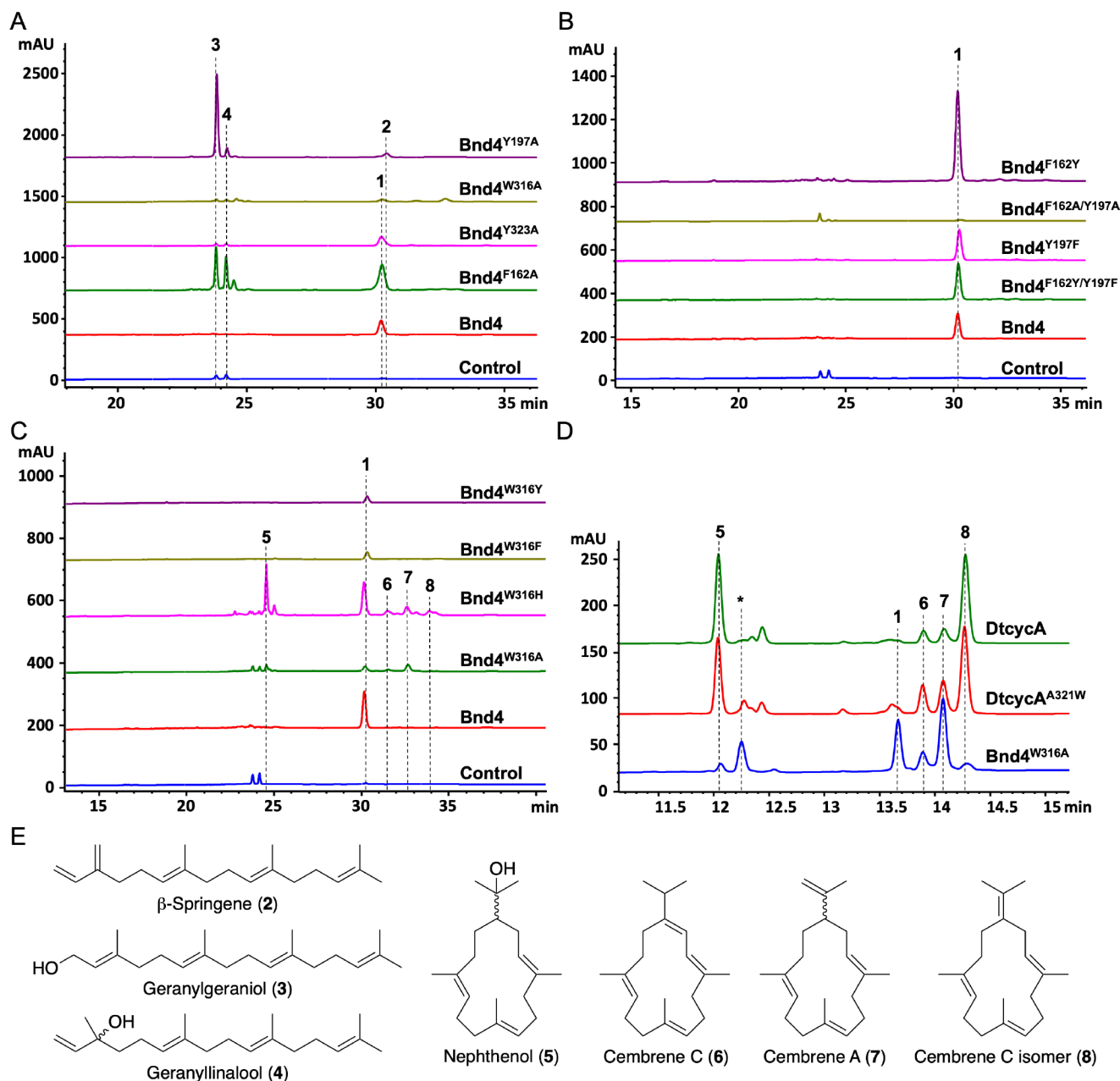


**Figure 2.** Mutation of the aromatic residues in Bnd4 alters its product profile. HPLC analyses of the Bnd4 variants in comparison with native Bnd4 (A–C) and the cembrene synthase DtcycA (D). Control reactions are no enzyme negative controls. (E) Structures of identified diterpene products. Enzyme products labeled with asterisks (\*) were uncharacterized.



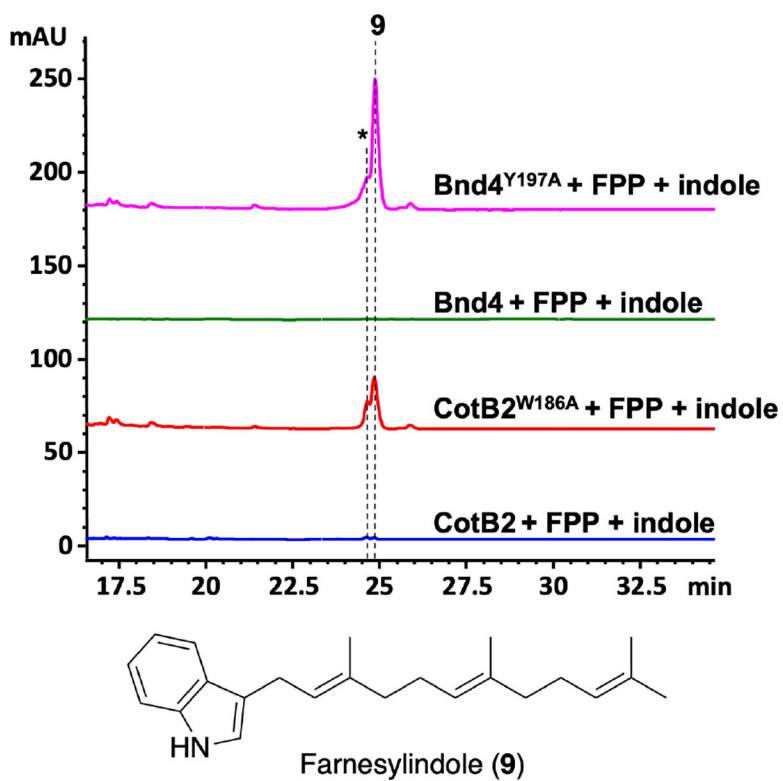


**Figure 3.** Prenylation activity of Bnd4 and CotB2 was expanded to farnesylation by engineering their active sites. Enzyme product labeled with an asterisk (\*) was not isolated.